JOURNAL OF THERMOPHYSICS AND HEAT TRANSFER
Vol. 8, No. 1, Jan.–March 1994

Analysis of Natural Convection in a Rotating Open Loop

Mark A. Stremler,* David R. Sawyers,† and Mihir Sen‡
University of Notre Dame, Notre Dame, Indiana 46556

This work deals with a one-dimensional analysis of a rotating open loop subjected to a uniform heat flux per unit length. Fluid temperature is fixed at the inlet of the loop. Flow is driven by buoyancy as well as by a pressure gradient. The criterion for onset of motion is first determined. Steady-state motion is then analyzed and is found to exhibit both a positive and a negative branch. Linear stability analysis is performed to determine regions in parameter space over which the flow is unstable. Parameters varied for this analysis are those corresponding to rotational velocity, heat flux, and a modified pressure difference across the loop. One or both velocities may be stable. It is also possible to have an oscillatory state coexist with a time-independent solution. A perturbation method is used to evaluate the effect of gravity on flow characteristics.

Nomenclature

A = peak-to-peak amplitude of gravity perturbed oscillation
a = real part of λ
b = imaginary part of λ
c = specific heat of fluid
D = diameter of tube
E = relative percentage error
F_b = buoyancy force per unit mass
F_p = pressure force per unit mass
F_v = viscous force per unit mass
f = friction factor
$f_\pm$ = transcendental function for eigenvalue determination
g = gravity
$\mathcal{J}$ = integrals
I = imaginary part of f
K = nondimensional thermal conductivity
k = thermal conductivity of fluid
L = total length of loop
m, n = constants for power law friction
p = pressure
Q = nondimensional heat flux per unit length
q = heat flux per unit length
R = real part of f
r = distance from axis of rotation
$\tilde{r}$ = nondimensional distance from axis of rotation
s = nondimensional distance along loop
T = fluid temperature
T_0 = fluid temperature at inlet
t = time
u = fluid velocity
V = nondimensional fluid velocity
W = scaled nondimensional fluid velocity
x = distance along loop
β = coefficient of thermal expansion
γ = nondimensional parameter
ΔP = nondimensional modified pressure difference across loop
$\Delta P'$ = nondimensional pressure difference across loop
Δp = pressure difference across loop
ε = perturbation parameter, $1/\Omega$
Θ = scaled nondimensional fluid temperature
θ = nondimensional fluid temperature
λ = eigenvalue
ν = kinematic viscosity of fluid
ρ = fluid density
ρ_0 = fluid density at reference temperature T_0
τ = nondimensional time
Ω = nondimensional speed of rotation
ω = speed of rotation

Superscripts
$\bar{}$ = time-independent state
$\hat{}$ = amplitude of perturbation
$*$ = scaled variables

Introduction

GAS turbine efficiencies are often limited by the maximum operating temperature of the turbine blades, which in turn is dictated by material properties. Cooling of turbine blades is therefore an important and active area of research. There are many ways in which modern gas turbines are cooled, one of them being the forcing of fluid through internal passages within the blades. In order to be effective, the fluid must pick up a large amount of heat which can induce substantial temperature changes. This is then reflected in density changes which, in conjunction with the large rotation speed of the blade, leads to a significant centrifugal force.

Internal cooling passages have complicated geometries in general,[1] and it is only possible to study flow and heat transfer in such a situation using numerical or experimental techniques. A review of convection in rotating systems has been presented by Kreith.[2] Some closed geometries have been studied analytically by Reiss and Magnan,[3] numerically by Yang et al.,[4] Torrance and Ladeinde,[5] and Chew,[6] and experimentally by Owen and Onur,[7] among others. Our purpose here is to approach the problem in a simplified manner to determine the important nondimensional parameters which govern the flow, as well as qualitative changes in system behavior as these parameters change. For this reason, we will make a one-dimensional assumption, even though the flow may be actually quite complicated.[8] Results obtained here are actually valid only for a flow path that is thin enough; however, they can be used as a basis for detailed computations in actual designs.

Received Aug. 7, 1992; revision received April 1, 1993; accepted for publication April 8, 1993.

*Currently Undergraduate Student, Rose-Hulman Institute of Technology, Terre Haute, IN 47803.
†Graduate Student, Department of Aerospace and Mechanical Engineering.
‡Associate Professor, Department of Aerospace and Mechanical Engineering.

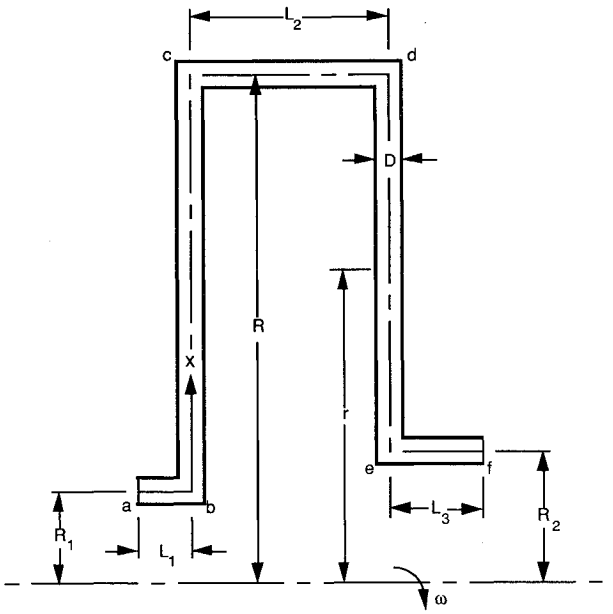

Fig. 1 Schematic of open-loop system.

Considerable work has also been done on one-dimensional modeling of loops with natural convection, especially in relation to closed systems. Reviews by Japikse[9] and Greif[10] can be consulted. Heating and cooling of different portions of a natural circulation loop may be through a prescribed heat flux[11] or wall temperature[12] boundary condition. The review by Sen et al.[13] covers the former case, and is the one that we will consider here. The open-loop model of Bau and Torrance[14] and Zhou and Bau[15] under mixed heating conditions is also relevant here since it considers the stability of the flow.

Some experiments on a rotating loop were conducted by Davis and Morris.[16] Mohamed and Bajaj[17] also studied convection in a closed loop of toroidal geometry under the action of rotation around a diameter. Their analysis used the one-dimensional approximation with a prescribed heat flux along the loop. Multiple steady states, a subcritical Hopf bifurcation, and chaotic states were found to be present.

Governing Equations

Consider a fluid-filled, open loop shown in Fig. 1 rotating about axis A-A with speed ω. The coordinate x will be measured along the length of the loop, starting from point a. The loop itself consists of a tube of D and L heated along its length by a heat flux $q(x)$. The flow is driven by Δp from a to f. The fluid may enter at either end, the inlet temperature being T_0. For simplicity, we will use a one-dimensional approximation with a mean fluid velocity and temperature at every section of the loop. This restricts us to a small diameter tube with negligible secondary circulation. We will also use the Boussinesq approximation and assume that all fluid properties are constant, with the exception of density varying linearly with temperature in the body force term.

Since the loop has a constant cross-sectional area, mass conservation dictates that u be a function of time only, i.e., $u = u(t)$. Energy balance yields the equation

$$c\rho_0 \frac{\pi D^2}{4}\left[\frac{\partial T}{\partial t} + u\frac{\partial T}{\partial x}\right] = q(x) + k\frac{\pi D^2}{4}\frac{\partial^2 T}{\partial x^2} \tag{1}$$

where $T(x, t)$ is temperature, and the last term represents axial conduction in the x direction.

By conservation of momentum, we have

$$\frac{du}{dt} = F_p + F_v + F_b \tag{2}$$

where F_p, F_v, and F_b are all in the x direction per unit mass of fluid. It can be shown that

$$F_p = -\frac{1}{\rho_0}\frac{\partial p}{\partial x}$$

Assuming a power-law friction factor of the form $f = m/(|u|D/\nu)^n$, the viscous force becomes

$$F_v = \frac{m\nu^n}{2D^{n+1}}\frac{u}{|u|^{n-1}} \tag{3}$$

The body force depends on centrifugal forces as well as g, and the variation of density must be taken into account. Therefore, we have

$$F_b = \begin{cases} 0 \quad \text{for} \quad a \le x < b; \quad c < x < d; \quad \text{and} \quad e < x \le f \\ (\rho/\rho_0)(r\omega^2 - g\cos\omega t) \quad \text{for} \quad b \le x \le c \\ (\rho/\rho_0)(-r\omega^2 + g\cos\omega t) \quad \text{for} \quad d \le x \le e \end{cases} \tag{4}$$

where we will assume that $\rho/\rho_0 = 1 - \beta(T - T_0)$. Time t is measured from an instant in which the loop is in a vertical position; r is measured outward from the axis of rotation.

We now introduce the following dimensionless parameters:

$$\tau = \frac{\nu}{DL}\left(\frac{mL}{2D}\right)^{1/n} t \qquad s = x/L$$

$$V = \frac{D}{\nu}\left(\frac{2D}{mL}\right)^{1/n} u \qquad \theta = \frac{\beta g L D^2}{\nu^2}\left(\frac{2D}{mL}\right)^{2/n}(T - T_0)$$

$$Q = \frac{4\beta g D L^2 q(s)}{\rho_0 c \pi \nu^3}\left(\frac{2D}{mL}\right)^{3/n} \qquad \Omega = \frac{DL}{\nu}\left(\frac{2D}{mL}\right)^{1/n}\omega$$

$$\gamma = \frac{\nu^2}{gLD^2}\left(\frac{mL}{2D}\right)^{2/n} \qquad \Delta P' = \frac{\Delta p}{gL\rho_0\gamma}$$

$$K = \frac{D}{L\nu\rho_0 c}\left(\frac{2D}{mL}\right)^{1/n} k \qquad \tilde{r} = r/L \tag{5}$$

We integrate the momentum equation along the length of the loop and use these parameters to get the nondimensional equation

$$\frac{dV}{d\tau} + \frac{V}{|V|^{n-1}} = \Delta P' + \Omega^2\int_b^c (1 - \gamma\theta) \times\left[\tilde{r} - \frac{\cos(\Omega\tau)}{\gamma\Omega^2}\right] ds - \Omega^2\int_d^e (1 - \gamma\theta) \times\left[\tilde{r} - \frac{\cos(\Omega\tau)}{\gamma\Omega^2}\right] ds \tag{6}$$

For the remainder of this article, we will consider a simple geometry which has horizontal portions $L_1 = L_2 = L_3 = 0$. For simplicity we also take $n = 1$, $m = 64$ which corresponds to Poiseuille flow in a pipe, and consider Q to be a constant over the length of the loop. The qualitative nature of the results will not be much different for other geometries, friction factors, or heat fluxes.

For large enough rotational speeds, gravity forces can be considered negligible compared to centrifugal forces; hence, we will assume that $\Omega >> [1/(\gamma\tilde{r})]^{1/2}$ for most of the article. The governing equations now become

$$\frac{\partial\theta}{\partial\tau} + V\frac{\partial\theta}{\partial s} = Q + K\frac{\partial^2\theta}{\partial s^2} \tag{7}$$

$$\frac{dV}{d\tau} + V = \Delta P - \Omega^2\gamma\left[\int_0^{1/2}\tilde{r}\theta\, ds - \int_{1/2}^1 \tilde{r}\theta\, ds\right] \tag{8}$$

where $\Delta P = \Delta P' + (1/2L^2)(R_1^2 - R_2^2)$. R_1 and R_2 are the radii at $s = 0$ and $s = 1$; ΔP is a pressure difference modified by centrifugal forces. Other parameters are Q, K, Ω, and a viscous parameter γ. ΔP, Q, and Ω will be considered to vary, while γ and K which depend on material and geometrical properties will be held constant. $V(\tau)$ and $\theta(s, \tau)$ are nondimensional velocity and temperature, respectively.

No-Flow Solution and Its Stability

We will first investigate the stability of the static solution which can be obtained when $\Delta P = 0$. For $\bar{V} = 0$, we get a temperature distribution from Eq. (7) to be

$$\bar{\theta} = (Q/2K)(1 - s)s \tag{9}$$

where $\bar{V}$ and $\bar{\theta}$ are time-independent solutions. We assume a perturbation of the form $V = \bar{V} + \hat{V}e^{\lambda\tau}$ and $\theta = \bar{\theta} + \hat{\theta}e^{\lambda\tau}$, where $\hat{V}$ and $\hat{\theta}$ are small. For stability, the real part of λ should be less than zero. Loss of stability for conductive systems is also normally through a zero imaginary part; a formal proof of this would have to follow a procedure such as that described by Chandrasekhar.[18] In the present case, however, we simply confirm numerically the existence of steady convective states after the no-flow solution becomes unstable. Thus, we can take $\lambda = 0$ to indicate loss of stability.

Equations (7) and (8) become

$$\hat{V} = -\Omega^2\gamma\left[\int_0^{1/2} s\hat{\theta}\,ds - \int_{1/2}^{1}(1 - s)\hat{\theta}\,ds\right] \tag{10}$$

$$K\frac{d^2\hat{\theta}}{ds^2} = \hat{V}\frac{d\bar{\theta}}{ds} \tag{11}$$

From these we find the condition that

$$\frac{K^2}{Q\Omega^2\gamma} \geq \frac{7}{5760} \tag{12}$$

for stability. The critical value of heat flux given by this expression is very small. Realistic values of Q will be much greater; for this reason we will ignore the rest state and neglect axial conduction in the rest of this article.

Steady Flow

Assuming that the system has reached a time-independent state, we have the equations

$$\bar{V}\frac{d\bar{\theta}}{ds} = Q \tag{13}$$

$$\bar{V} = \Delta P - \Omega^2\gamma\left[\int_0^{1/2} s\bar{\theta}\,ds - \int_{1/2}^{1}(1 - s)\bar{\theta}\,ds\right] \tag{14}$$

where $\bar{V}$ and $\bar{\theta}(s)$ denote steady-state fluid velocity and temperature, respectively. The boundary condition on the temperature corresponds to that at the inlet. For $\bar{V} > 0$, the inlet is at $s = 0$, but for $\bar{V} < 0$, the inlet is at $s = 1$. Thus, we have $\bar{\theta}(0) = 0$ for $\bar{V} > 0$, and $\bar{\theta}(1) = 0$ for $\bar{V} < 0$.

For $\bar{V} < 0$, integration of Eq. (13) gives the temperature profile

$$\bar{\theta} = (Q/\bar{V})s \tag{15}$$

Substituting into Eq. (14) and integrating leads to the steady-state fluid velocity

$$\bar{V} = \tfrac{1}{2}[\Delta P + \sqrt{\Delta P^2 + (\gamma\Omega^2 Q/6)}] \tag{16}$$

The $\bar{V} < 0$ solutions can be similarly found to be

$$\bar{\theta} = -(Q/\bar{V})(1 - s) \tag{17}$$

$$\bar{V} = \tfrac{1}{2}[\Delta P - \sqrt{\Delta P^2 + (\gamma\Omega^2 Q/6)}] \tag{18}$$

Figures 2a–c show the steady-state fluid velocity as a function of governing parameters ΔP, Q, and Ω. In each case we see that there are two velocities possible, one in the positive,

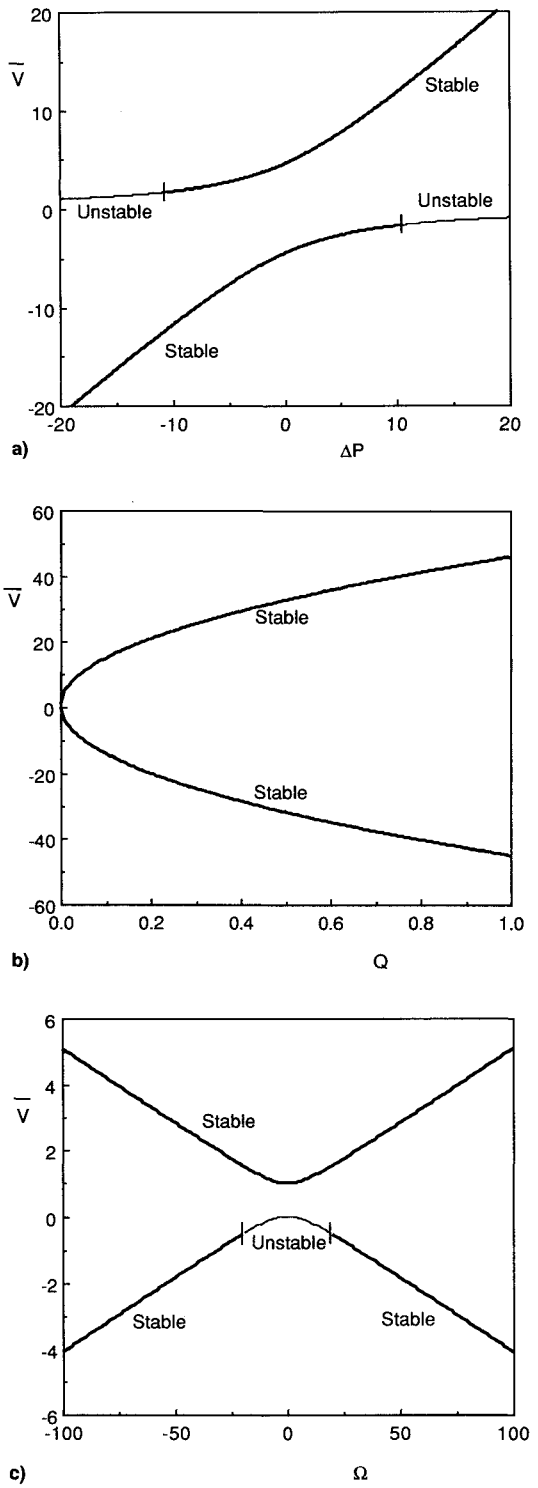

Fig. 2 a) Steady-state velocity as a function of modified pressure difference, with $\gamma = 5$, $Q = 0.01$, $\Omega = 100$; b) steady-state velocity as a function of heat flux with $\gamma = 5$, $\Delta P = 1$, $\Omega = 100$; and c) steady-state velocity as a function of rotational velocity with $\gamma = 5$, $\Delta P = 1$, $Q = 0.01$.

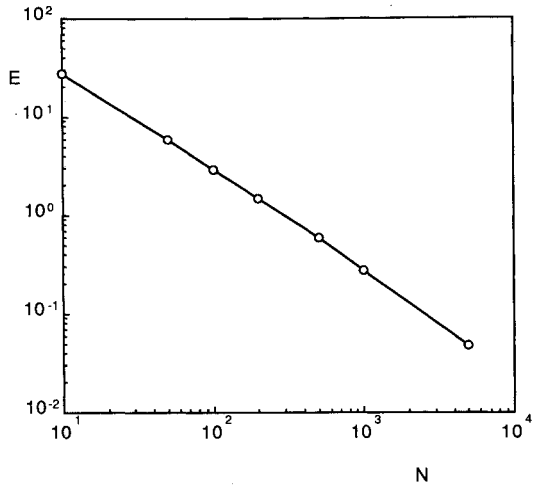

Fig. 3 Convergence of numerical scheme with $\gamma = 1$, $Q = 1$, $\Omega = 50$.

and another in the negative direction. The one that will appear in the dynamical problem will depend on initial conditions as well as stability of the solutions. In the figures the stable and unstable velocities are denoted by thick and thin lines, respectively, determined from a stability analysis to be presented later on.

Numerical Solution of Governing Equations

It is possible to study the behavior of the velocity and temperature field as a function of time through numerical solution of the governing equations. We use here an implicit time marching method. First, energy Eq. (7) with $K = 0$ is solved exactly as[19]

$$d\tau = \frac{ds}{V(\tau)} = \frac{d\theta(s, \tau)}{Q} \tag{19}$$

We divide the loop into N segments so that the length of each segment is $\Delta s = 1/N$. The time step $\Delta\tau$ is taken to be the interval in which the fluid moves a distance Δs. From Eq. (19) we have $\Delta\tau = \Delta s/V(\tau)$. At time $\tau + \Delta\tau$, the temperature field, also from Eq. (19), is

$$\theta(s \pm \Delta s, \tau + \Delta\tau) = \theta(s, \tau) + Q\Delta\tau \tag{20}$$

where the positive sign is for $V > 0$, and the negative for $V < 0$. We can now use the momentum Eq. (8) to find $V(\tau + \Delta\tau)$, where the integrals in

$$\mathcal{I}(\theta) = \int_0^{1/2} \tilde{r}\theta(s, \tau + \Delta\tau)\, ds - \int_{1/2}^{1} \tilde{r}\theta(s, \tau + \Delta\tau)\, ds \tag{21}$$

are evaluated using the trapezoidal rule. Thus

$$V(\tau + \Delta\tau) = [\Delta P - \Omega^2\gamma\mathcal{I} - V(\tau + \Delta\tau)]\Delta\tau + V(\tau) \tag{22}$$

which is iterated to obtain a value for $V(\tau + \Delta\tau)$. The iteration process is started by letting $V(\tau + \Delta\tau) = V(\tau)$ on the right side.

Errors in the numerical scheme are not introduced in Eq. (19), which is exact, but in its discrete form [Eq. (20)] as well as in the evaluation of the integrals in Eq. (21). The accuracy depends on N. The error in the steady-state numerical solution can be quantified by comparing it with analytical solution. Figure 3 shows that E is proportional to $1/N$. In the numerical results shown here, values of $N \geq 500$ were used.

Linear Stability of Steady Flow

Conditions for stability of steady solutions $\bar{V}$ and $\bar{\theta}(s)$ will now be determined. We assume perturbations of the form $V(\tau) = \bar{V} + \hat{V}e^{\lambda\tau}$ and $\theta(s, \tau) = \bar{\theta}(s) + \hat{\theta}(s)e^{\lambda\tau}$, where $\hat{V}$ and $\hat{\theta}$ are small. Applying these to Eqs. (7) and (8) and linearizing, we get

$$\frac{d\hat{\theta}}{ds} + \frac{\lambda}{\bar{V}}\hat{\theta} = -\frac{\hat{V}}{\bar{V}}\frac{d\bar{\theta}}{ds} \tag{23}$$

$$\hat{V}(\lambda + 1) = -\Omega^2\gamma\left[\int_0^{1/2} s\hat{\theta}\, ds - \int_{1/2}^{1} (1 - s)\hat{\theta}\, ds\right] \tag{24}$$

for $\bar{V} > 0$. Using boundary condition $\hat{\theta}(0) = 0$, the solution of Eq. (23) is

$$\hat{\theta} = \frac{\hat{V}Q}{\lambda\bar{V}}[\exp(-\lambda s/\bar{V}) - 1] \tag{25}$$

Substituting into Eq. (24) and integrating, we get the eigenvalue equation

$$f_+(\Delta P, \gamma, \Omega, Q) = \frac{1}{\lambda^3}[\bar{V}\exp(-\lambda/\bar{V}) + \lambda\exp(-\lambda/2\bar{V}) - \bar{V}] - \frac{\lambda + 1}{\gamma\Omega^2 Q} = 0 \tag{26}$$

Similarly, for $\bar{V} < 0$, we have

$$f_-(\Delta P, \gamma, \Omega, Q) = \frac{1}{\lambda^3}[-\bar{V}\exp(-\lambda/\bar{V}) + \lambda\exp(\lambda/2\bar{V}) + \bar{V}] - \frac{\lambda + 1}{\gamma\Omega^2 Q} = 0 \tag{27}$$

With a given a set of parameters, these transcendental equations can be numerically solved for λ. To do this, first we let

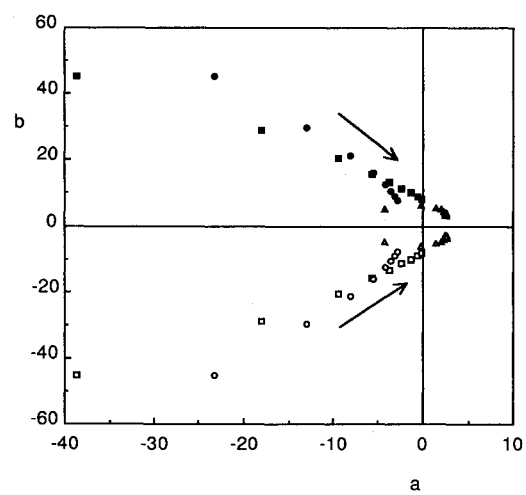

Fig. 4 Path of eigenvalues with variation of modified pressure difference with $\gamma = 5$, $Q = 0.01$, $\Omega = 100$.

$\lambda = a + ib$ and then separate f_+ into its real and imaginary parts, $R(a, b)$ and $I(a, b)$, where

$$R(a, b) = \frac{1}{(a^2 + b^2)^3}\{\bar{V}\exp(-a/\bar{V})(a^2 - 3b^2)a\cos(b/\bar{V}) + a\exp(-a/2\bar{V})(a^2 - 3b^2)[a\cos(b/2\bar{V}) + b\sin(b/2\bar{V})] - a\bar{V}(a^2 - 3b^2) + \bar{V}\exp(-a/\bar{V})(b^2 - 3a^2)b\sin(b/\bar{V}) - b\exp(-a/2\bar{V})(b^2 - 3a^2)[b\cos(b/2\bar{V}) - a\sin(b/2\bar{V})]\} - \frac{a + 1}{\gamma\Omega^2 Q} = 0 \quad (28)$$

$$I(a, b) = \frac{1}{(a^2 + b^2)^3}\{-\bar{V}\exp(-a/\bar{V})(a^2 - 3b^2)a\sin(b/\bar{V}) + a\exp(-a/2\bar{V})(a^2 - 3b^2)[b\cos(b/2\bar{V}) - a\sin(b/2\bar{V})] - b\bar{V}(b^2 - 3b^2) + \bar{V}\exp(-a/\bar{V})(b^2 - 3a^2)b\cos(b/\bar{V}) + b\exp(-a/2\bar{V})(b^2 - 3a^2)[a\cos(b/2\bar{V}) + b\sin(b/2\bar{V})]\} - \frac{b + 1}{\gamma\Omega^2 Q} = 0 \quad (29)$$

We now have two equations, $R(a, b) = 0$ and $I(a, b) = 0$, the roots of which correspond to eigenvalues. A numerical search for the roots was begun by creating a uniform grid in the (a, b) plane and determining the signs of R and I at each grid point. Once this was found, it was used as an initial guess for a two-dimensional Newton-Raphson scheme which enabled convergence to an eigenvalue. In this way all eigenvalues within a given region of the complex plane can be determined for specified values of the parameters. On making a small change in the value of a parameter, the new locations of the eigenvalues are found by using the Newton-Raphson scheme with the previous eigenvalues as an initial guess.

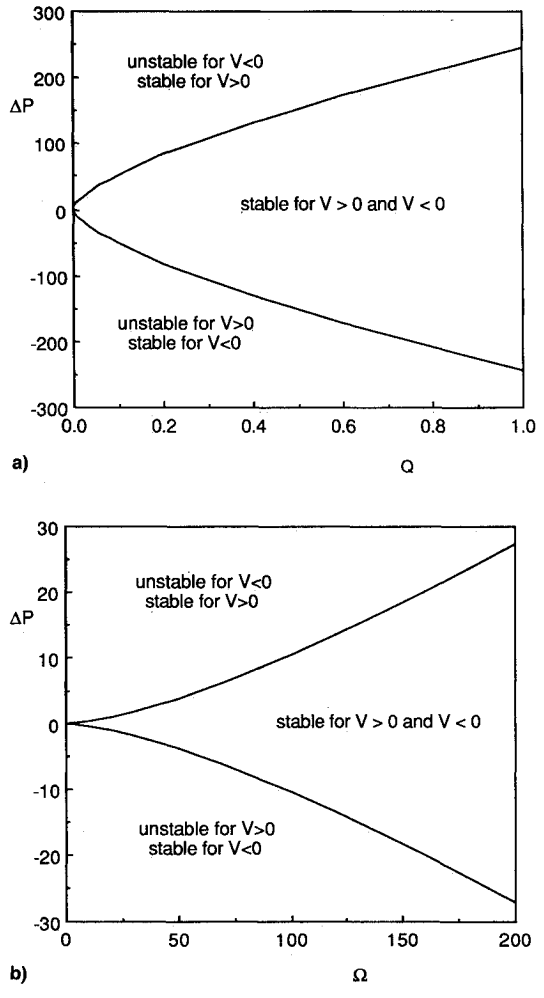

Fig. 5 Stability boundaries with a) $\gamma = 5$, $\Omega = 100$ and b) $\gamma = 5$, $Q = 0.01$.

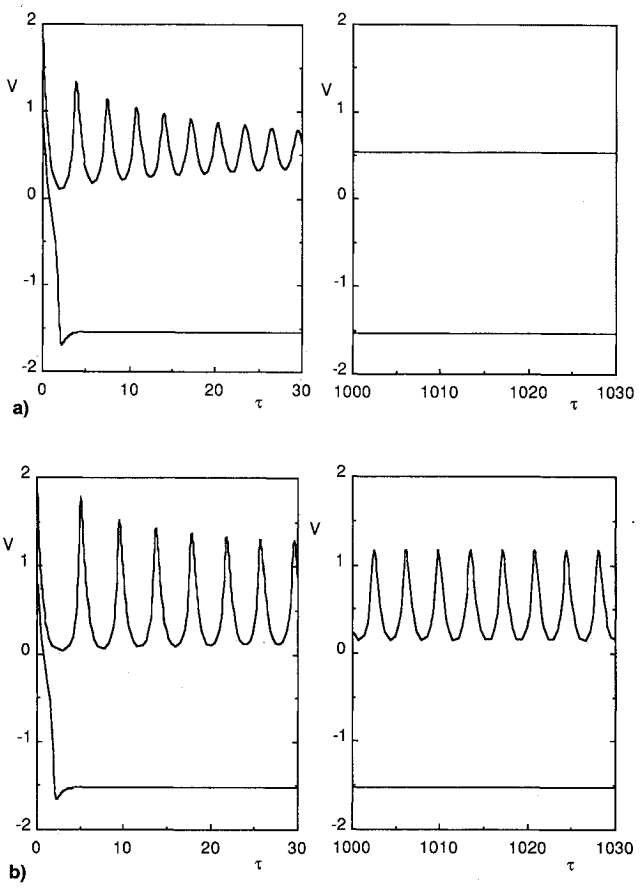

Fig. 6 a) Both time-independent solutions stable with $\gamma = 5$, $Q = 0.01$, $\Delta P = -1$, $\Omega = 20$ and b) only one time-independent solution stable with $\gamma = 5$, $Q = 0.01$, $\Delta P = -1$, $\Omega = 19.5$.

The path of each eigenvalue can be traced on the (a, b) plane as parameters are varied. As an example, Fig. 4 shows the behavior of the eigenvalues for different ΔP, while Ω and Q are kept fixed. Each symbol represents a different eigenvalue, the arrows indicating the general direction of motion of the eigenvalues as ΔP is increased (or decreased) for $V < 0$ (or for $V > 0$) in steps of 100. The real part of λ determines the stability of the steady state. At a certain value of ΔP, an eigenvalue pair crosses over from the stable side with $a < 0$ to the unstable side with $a > 0$. In a similar manner Ω and Q can be varied. It is found that increasing Ω or Q causes one branch of the steady state to go from unstable to stable.

Figures 5a and 5b show boundaries at which instability occurs. For certain parameter values both steady states are stable, while for other values only one is stable. In each case instability is manifested by a conjugate eigenvalue pair crossing the imaginary axis. This Hopf bifurcation produces a stable finite amplitude oscillation which can be numerically computed. To indicate what happens at onset of instability, we have shown numerically obtained velocity vs time traces in Figs. 6a and 6b. In Fig. 6a, parameter values are such that the system is barely on the stable side of the boundary. The two initial conditions chosen eventually converge to two different steady states that are both stable. In Fig. 6b, in contrast, one solution converges to a steady solution, while the other is attracted to a limit cycle. In this region of parameter space, a time-independent solution and a constant amplitude oscil-

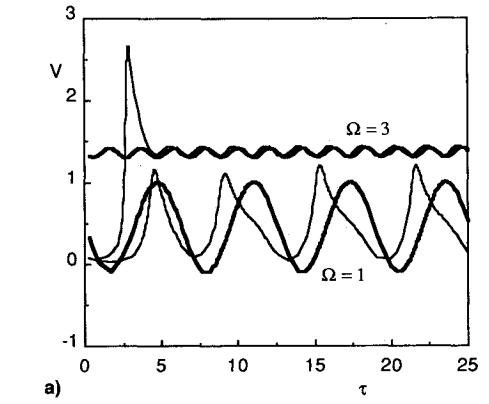

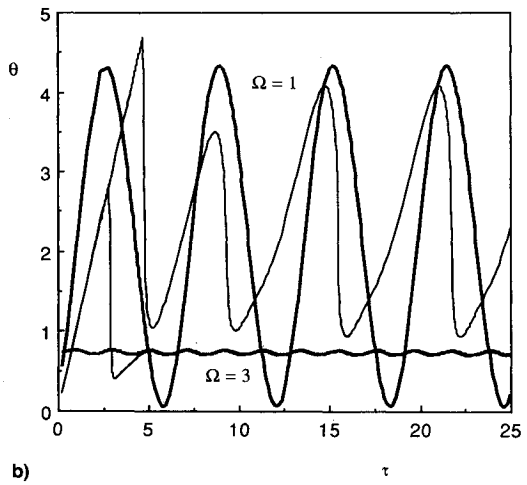

Fig. 7 a) Time-dependent velocity for gravity perturbed flow with $\gamma = 5$, $Q = 1$, $\Delta P = 0$ and b) time-dependent exit temperature for gravity perturbed flow with $\gamma = 5$, $Q = 1$, $\Delta P = 0$.

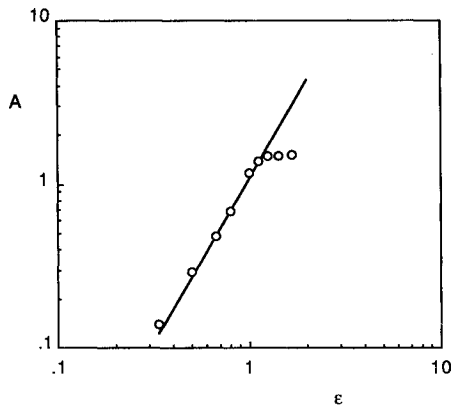

Fig. 8 Amplitude of velocity oscillations with $\gamma = 5$, $Q = 1$, $\Delta P = 0$. Straight line: perturbation solution, points: numerical.

lation are both seen to coexist. The latter appears to be stable for the time periods up to which integration was performed. This is in contrast to the nonrotating open loop studied by Bau and Torrance[14] and by Zhou and Bau,[15] where the oscillary solution grows in amplitude until the flow finally reverses direction.

Effect of Gravity

So far we have neglected the effect of gravity in comparison to centrifugal force. Gravity is a small periodic forcing on the system; we will determine its effect on the steady state using a perturbation method. For this purpose we scale the variables appropriately, introducing $w = V/\Omega$, $\theta^* = \Omega\theta$, $\tau^* = \Omega\tau$, as well as a perturbation parameter $\varepsilon = 1/\Omega$, where ε is small. We then allow gravity to perturb the velocity and temperature from steady state; thus, $w = \bar{w} + W$ and $\theta^* = \theta^* + \Theta$, where $\bar{w}$ and $\bar{\theta}$ are the steady states. This change of variables causes Eqs. (7) and (8) with $K = 0$ to become

$$\frac{\partial \Theta}{\partial \tau^*} + \bar{w}\frac{\partial \Theta}{\partial s} + W\frac{\partial \Theta}{\partial s} + \frac{WQ}{\bar{w}} = 0 \tag{30}$$

$$\frac{dW}{d\tau^*} + \varepsilon W = -\varepsilon\gamma\left[\int_0^{1/2} s\Theta\, ds - \int_{1/2}^{1} \Theta\, ds\right] + \varepsilon^3 \cos\tau^*\left[\int_0^{1/2} \Theta\, ds - \int_{1/2}^{1} \Theta\, ds\right] - \varepsilon^3 \frac{Q}{4\bar{w}} \cos\tau^* \tag{31}$$

We can then expand W and Θ as

$$W(\tau^*) = \varepsilon W_1(\tau^*) + \varepsilon^2 W_2(\tau^*) + \varepsilon^3 W_3(\tau^*) + O(\varepsilon^4) \tag{32}$$

$$\Theta(s, \tau^*) = \varepsilon\Theta_1(s, \tau^*) + \varepsilon^2\Theta_2(s, \tau^*) + \varepsilon^3\Theta_3(s, \tau^*) + O(\varepsilon^4) \tag{33}$$

Boundary conditions on temperature are $\Theta_i(0, \tau^*) = 0$ ($i = 1, 2, \ldots$). Substituting the expansions into Eqs. (30) and (31) and collecting terms of $O(\varepsilon)$ and $O(\varepsilon^2)$, we find that W_1, Θ_1, W_2, and Θ^2 are all zero.

Terms of $O(\varepsilon^3)$ produce

$$\frac{dW_3}{d\tau^*} = -\frac{Q}{4\bar{w}} \cos\tau^* \tag{34}$$

$$\frac{\partial \Theta_3}{\partial \tau^*} + \bar{w}\frac{\partial \Theta_3}{\partial s} = -\frac{W_3 Q}{\bar{w}} \tag{35}$$

By solving these equations for W_3 and Θ_3, and converting back to our original nondimensional parameters, we are able to obtain, to lowest-order approximation, solutions for velocity and temperature as perturbed from steady state by gravity. These are

$$V(\tau) = \bar{V}\left(1 - \frac{Q}{4\Omega\bar{V}^2} \sin\Omega\tau\right) + \text{h.o.t.} \tag{36}$$

$$\theta(s, \tau) = \bar{\theta}\left\{1 + \frac{Q}{4\Omega\bar{V}^2}[\cos(\Omega\tau - \Omega s/\bar{V}) - \cos\Omega\tau]\right\} + \text{h.o.t.} \tag{37}$$

Figure 7a compares the velocity obtained above to that found numerically using $N = 1000$. Two different Ω are used. An increase in rotational velocity both improves the accuracy of the perturbation solution as well as decreases the effect of gravity. In Fig. 7b we see a similar effect on fluid temperature at the exit of the loop. Both figures indicate that the perturbation method provides a fairly good solution for large time.

We can also look at A, obtained numerically and by the perturbation solution. Figure 8 shows that they compare very well, until about $\varepsilon = 1$, where the perturbation method breaks down.

Conclusions

The analysis presented here can be used to determine the qualitative characteristics of flow in a rotating loop. The parameter values chosen are realistic. In general, the analysis predicts two steady velocities: one is in the direction of the modified pressure gradient, while the other is against it. For some values of the governing parameters, both these solutions

are stable, while for others only one is stable. Oscillatory solutions are found on crossing the stability boundary. The effect of gravity is small for large rotational rates, its only effect being to provide a time-dependent driving force leading to small amplitude oscillations.

Acknowledgment

We thank the Indiana Space Grant Consortium for the sponsorship of M. Stremler.

References

[1]Smith, M. K. D., and Hannis, J. M., "The Design and Testing of Air-Cooled Blading for an Industrial Gas Turbine," *Journal of Engineering for Power*, Vol. 105, No. 3, 1983, pp. 466–473.

[2]Kreith, F., "Convection Heat Transfer in Rotating Systems," *Advances in Heat Transfer*, Vol. 5, Academic Press, New York, 1968, pp. 129–251.

[3]Reiss, E. L., and Magnan, J. F., "Rotating Thermal Convection: Neosteady and Neoperiodic Solutions," *Journal on Applied Mathematics*, Vol. 48, No. 4, 1988, pp. 808–827.

[4]Yang, K. T., Lloyd, J. R., and Yang, H. Q., "Rotational Effects on Natural Convection in a Horizontal Cylinder," *AIChE Journal*, Vol. 34, No. 10, 1988, pp. 1627–1633.

[5]Torrance, K. E., and Ladeinde, F., "Convection in a Rotating, Horizontal Cylinder with Radial and Normal Gravity Forces," *Journal of Fluid Mechanics*, Vol. 228, 1991, pp. 361–385.

[6]Chew, J. W., "Computation of Forced Laminar Convection in Rotating Cavities," *Journal of Heat Transfer*, Vol. 107, No. 2, 1985, pp. 277–282.

[7]Owen, J. M., and Onur, H. S., "Convective Heat Transfer in a Rotating Cylindrical Cavity," *Journal of Engineering for Power*, Vol. 105, No. 2, 1983, pp. 265–271.

[8]Morris, W. D., *Heat Transfer and Fluid Flow in Rotating Coolant Channels*, Research Studies Press, Chichester, England, UK, 1981.

[9]Japikse, D., "Advances in Thermosyphon Technology," *Advances in Heat Transfer*, Vol. 9, Academic Press, New York, 1973, pp. 1–111.

[10]Greif, R., "Natural Circulation Loops," *Journal of Heat Transfer*, Vol. 110, No. 4B, 1988, pp. 1243–1258.

[11]Sen, M., Ramos, E., and Treviño, C., "The Toroidal Thermosyphon with Known Heat Flux," *International Journal of Heat and Mass Transfer*, Vol. 28, No. 1, 1985, pp. 219–233.

[12]Yorke, J. A., and Yorke, E. D., "Chaotic Behavior and Fluid Dynamics," *Hydrodynamic Instabilities and the Transition to Turbulence*, edited by H. L. Swinney and J. P. Gollub, 2nd ed., Springer-Verlag, Berlin, 1985, pp. 77–95.

[13]Sen, M., Treviño, C., and Ramos, E., "One-Dimensional Modeling of Thermosyphons with Known Heat Flux," *Trends in Heat, Mass and Momentum Transfer* (to be published).

[14]Bau, H. H., and Torrance, K. E., "On the Stability and Flow Reversal of an Asymmetrically Heated Open Convection Loop," *Journal of Fluid Mechanics*, Vol. 106, 1981, pp. 417–433.

[15]Zhou, K.-Y., and Bau, H. H., "On the Stability and Flow Reversal of Pressure-Driven Flow in an Asymmetrically Heated U-Shaped Tube," *Journal of Heat Transfer*, Vol. 107, No. 1, 1985, pp. 112–117.

[16]Davis, T. H., and Morris, W. D., "Heat Transfer Characteristics of a Closed Loop Rotating Thermosyphon," *Proceedings of the Third International Heat Transfer Conference* (Chicago, IL), Vol. 2, AIChE, New York, 1966, pp. 172–181.

[17]Mohamad, A. A., and Bajaj, A. K., "Dynamics of a Spinning Toroidal Thermosyphon," American Society of Mechanical Engineers Paper 91-HT-23, 1991.

[18]Chandrasekhar, S., *Hydrodynamic and Hydromagnetic Stability*, Dover, New York, 1961.

[19]Sneddon, I., *Partial Differential Equations*, McGraw-Hill, New York, 1957.